Chemosphere 287 (2022) 131975

Contents lists available at ScienceDirect

Chemosphere

journal homepage: www.elsevier.com/locate/chemosphere

Biofilm carrier type affects biogenic sulfur-driven denitrification performance and microbial community dynamics in moving-bed biofilm reactors

Anastasiia Kostrytsia [a,*], Stefano Papirio [b,c], Murod Khodzhaev [d], Liam Morrison [e], Gavin Collins [f], Piet N.L. Lens [d], Umer Zeeshan Ijaz [g,**], Giovanni Esposito [b]

[a] Department of Civil and Mechanical Engineering, University of Cassino and Southern Lazio, via Di Biasio 43, 03043, Cassino (FR), Italy
[b] Department of Civil, Architectural and Environmental Engineering, University of Naples Federico II, via Claudio 21, 80125, Naples, Italy
[c] Task Force on Microbiome Studies, University of Naples Federico II, 80138, Naples, Italy
[d] IHE Delft Institute for Water Education, PO Box 3015, 2601 DA, Delft, the Netherlands
[e] Earth and Ocean Sciences, School of Natural Sciences and Ryan Institute, National University of Ireland Galway, University Road, Galway, H91 TK33, Ireland
[f] Microbial Communities Laboratory, School of Natural Sciences and Ryan Institute, National University of Ireland Galway, University Road, Galway, H91 TK33, Ireland
[g] School of Engineering, University of Glasgow, Oakfield Avenue, Glasgow, G12 8LT, United Kingdom

HIGHLIGHTS

- Denitrification rate and NO_2^- accumulation differed depending on the carrier type.
- The biofilm mass on K1 carriers was 4.8 times higher than that on Z-200 supports.
- The same species were present in K and Z studies but they differed in abundances.
- The active microbial community varied significantly over time in MBBR with Z-200.
- More microorganisms were associated with process failure for Z-200 than K1 biofilms.

GRAPHICAL ABSTRACT

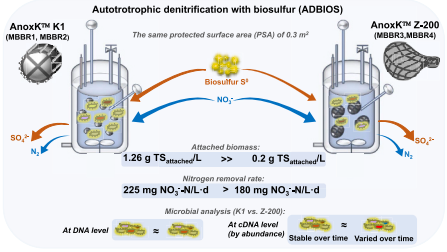

ARTICLE INFO

Handling Editor: A ADALBERTO NOYOLA

Keywords:
Autotrophic denitrification
Biogenic sulfur
Nitrite
Moving-bed biofilm reactor

ABSTRACT

Autotrophic denitrification with biosulfur (ADBIOS) provides a sustainable technological solution for biological nitrogen removal from wastewater driven by biogenic S^0, derived from biogas desulfurization. In this study, the effect of different biofilm carriers (conventional AnoxK™ 1 and Z-200 with a pre-defined maximum biofilm thickness) on ADBIOS performance and microbiomics was investigated in duplicate moving bed-biofilm reactors (MBBRs). The MBBRs were operated parallelly in continuous mode for 309 days, whilst gradually decreasing the hydraulic retention time (HRT) from 72 to 21 h, and biosulfur was either pumped in suspension (days 92–223) or supplied in powder form. Highest nitrate removal rates were approximately 225 (±11) mg/L·d and 180 (±7) mg

* Corresponding authors. Infrastructure and Environment, School of Engineering, University of Glasgow, Rankine Building, Oakfield Avenue 79-85, Glasgow, G12 8LT, UK.
** Corresponding author. Infrastructure and Environment, School of Engineering, University of Glasgow, Rankine Building, Oakfield Avenue 79-85, Glasgow, G12 8LT, UK.
E-mail addresses: Anastasiia.Kostrytsia@glasgow.ac.uk (A. Kostrytsia), umer.ijaz@glasgow.ac.uk (U.Z. Ijaz).

https://doi.org/10.1016/j.chemosphere.2021.131975
Received 18 April 2021; Received in revised form 23 July 2021; Accepted 19 August 2021
Available online 20 August 2021

Z-200 carrier
Microbial profile

NO_3^--N/L·d in the MBBRs operated with K1 and Z-200 carriers, respectively. Despite having the same protected surface area for biofilm development in each MBBR, the biomass attached onto the K1 carrier was 4.8-fold more than that on the Z-200 carrier, with part of the biogenic S^0 kept in the biofilm. The microbial communities of K1 and Z-200 biofilms could also be considered similar at cDNA level in terms of abundance ($R = 0.953$ with $p = 0.042$). A relatively stable microbial community was formed on K1 carriers, while the active portion of the microbial community varied significantly over time in the MBBRs using Z-200 carriers.

1. Introduction

The contamination of water resources is of serious environmental concern, mainly due to industrialization and the rapidly increasing human population. Conventionally, nitrate (NO_3^-) pollution of surface waters is prevented by biological denitrification of wastewaters mediated by heterotrophic microorganisms using organic compounds as electron donors. However, some NO_3^--rich wastewaters with low organic carbon content, such as those generated from mining, fertilizer and textile industries, thus require external sources of carbon to support complete denitrification (Sahinkaya et al., 2014). Therefore, for wastewaters with a low C/N ratio, the application of autotrophic denitrification is emerging as an attractive solution due to inherently lower costs and higher denitrification efficiency (Huang et al., 2021; Namburath et al., 2020; Peng et al., 2021).

Chemically synthesized elemental sulfur (S^0) has been widely used as an electron donor for autotrophic denitrification, but its low water solubility resulted in reduced process rates (Christianson et al., 2015; Kostrytsia et al., 2018a;b; Sahinkaya et al., 2014). Alternatvely, biogenic S^0 (or biosulfur) has been recently proposed for sustainable denitrification applications (Kostrytsia et al., 2018c; Ucar et al., 2020; 2021). Biosulfur is a by-product of well-established biological gas desulfurization technology (Thiopaq®, Paques BV, The Netherlands). Specifically, biogenic S^0 globules (2–40 μm) are produced as a result of incomplete sulfide oxidation by various S-oxidizing microorganisms, and are hydrophilic (Janssen et al., 1999; Kamyshny et al., 2009; Kostrytsia et al., 2018c). Such hydrophobicity makes biogenic S^0 particularly reactive and bioavailable, and preliminary experiments on autotrophic denitrification with biosulfur (ADBIOS) in batch microcosms showed 10-times faster denitrification kinetics (Kostrytsia et al., 2018c) compared to those obtained with chemically synthesized S^0 (Huiliñir et al., 2020; Kostrytsia et al., 2018a). Therefore, further studies on the ADBIOS process are of great interest, mainly if aimed at further increasing the bioprocess rates in continuous-flow bioreactors.

Among the main bioreactor configurations used for denitrification purposes, attached-growth systems allow the retention of microorganisms in the form of a biofilm, thus reducing the sensitivity of microbes to unfavorable environmental conditions and facilitating shorter hydraulic retention times (HRTs) (Ødegaard et al., 1994). Moreover, immobilized-cell bioreactors allow decoupling of the HRT from the sludge retention time (SRT), which can be maintained long enough to enable the development and retention of slow-growing microorganisms, such as autotrophic denitrifiers (Lemaire et al., 2013). The performance of a moving-bed biofilm reactor MBBR, as a biofilm-based system, relies on the hydrodynamics within the reactor, biofilm thickness, growth and activity of the biofilm (Bassin et al., 2016), which can be affected by the type of biofilm carrier. MBBR carriers are designed to have a large protected surface area (PSA), which has been characterized as the carrier surface area available for biofilm growth in a protected environment (Ødegaard et al., 1994; Wang et al., 2021).

The original and most widely used biofilm carrier AnoxK™ 1 (formerly known as AnoxKaldnes™ K1) (K1) has been the preferred biofilm carrier design to provide a large PSA for the development of biofilms in the inner part of the cylindrical-shaped carrier, which is not subjected to direct collision with other carriers and thus protected from hydraulic shear (Ødegaard et al., 1994). Diffusion, caused by differences in substrate and metabolite concentrations, is the main transport mechanism for MBBR biofilms (Piculell et al., 2016). However, thick K1 biofilms are only partially penetrated by substrates and only microorganisms located in outer fractions of the biofilm are usually active (Boltz and Daigger, 2010). To control biofilm thickness based on the carrier surface area, the novel AnoxK™ Z-carrier with a grid of defined height, was designed to allow biofilm growth on the outside of the carrier but in a protected environment (Welander and Piculell, 2016). Due to scouring from other carriers (abrasion), such biofilms cannot grow higher than the grid height, and so biofilm thickness is controlled for better substrate diffusion into the biofilm.

The role of biofilm carrier type in optimization of the ADBIOS process and in the development of the associated microbial community, has never been investigated. In addition, to the best of our knowledge, biogenic S^0 has never been tested as a substrate for denitrification in continuous-flow MBBRs. Therefore, the present study aims to offer new insights and promising perspectives in view of an efficient and robust performance of ADBIOS of high-strength NO_3^- wastewaters. Duplicate MBBRs were operated and filled with respectively the classical K1 and the recently proposed AnoxK™ Z-200 (Z-200) biofilm carriers. The main objectives of this study were to: (i) compare the ADBIOS performance in MBBRs operated with the two different biofilm carriers, (ii) study the main physico-chemical characteristics of the biofilm on each carrier type, (iii) identify the dominant microbial taxa in the biofilm and (iv) describe the structure of the active portion of the microbial community.

2. Materials and methods

2.1. Experimental set-up

The experimental set-up consisted of four identical, double-walled, glass MBBRs each with a working volume of 1.5 L (Figure S1). Two types of biofilm carrier were used: (1) the original and most widely used MBBR K1 carrier, shaped as a small cylinder with a cross inside (10 mm diameter; 7 mm length); and (2) the recently proposed saddle-shaped Z-200 carrier (30 mm diameter; 200 μm grid wall height) (Figure S1). The twin reactors, MBBR1 and MBBR2, were 40% filled ($V_{carrier}/V_{reactor}$) with K1 carriers, while the twin MBBR3 and MBBR4 reactors were 20% filled ($V_{carrier}/V_{reactor}$) with Z-200 carriers (Figure S1). The media-filling fractions guaranteed the same PSA of 0.3 m^2 and good mixing conditions in each reactor, as recommended by Piculell et al. (2016).

The temperature in the MBBRs was maintained at 30 (±2) °C by means of a heating circulator (F12-ED, Julabo GmbH, Germany). pH, dissolved oxygen (DO) and oxidation-reduction potential (ORP) values were monitored daily. Each MBBR was placed on a magnetic stirrer (M2-A, Argo Lab, Italy), allowing agitation at 300 rpm, i.e. similar to that used in a previous study (Kostrytsia et al., 2018c). Peristaltic pumps (Minipuls 3, Gilson, USA) were used to feed the synthetic wastewater (Section 2.2) to the MBBRs and pump out the effluent.

2.2. Inoculum and medium

The MBBRs were inoculated with activated sludge (10% of the entire MBBR volume) obtained from the denitrifying tank of a municipal

wastewater treatment plant (Cassino, Italy) and having a total solid concentration of approximately 4200 mg/L. The microbial composition of the inoculum was characterized previously (Kostrytsia et al., 2018a). The influent NO_3^- concentration was 225 mg NO_3^--N/L, i.e. similar to that used in a previous batch study on ADBIOS to simulate industrial wastewater with low C/N ratio (Kostrytsia et al., 2018c). $NaHCO_3$ (2.0 g/L) was supplied as buffer and a carbon source to each reactor. The distilled water basal medium also contained (per liter): 0.4 g NH_4Cl, 0.6 g KH_2PO_4, 1.6 g K_2HPO_4 and 0.021 g $MgCl_2{\cdot}6H_2O$. A trace elements solution was added (10 mL/L) as reported elsewhere (Kostrytsia et al., 2018c). The feed was maintained at pH 8.5 (±0.3) and at 25 °C.

Biogenic S^0 (Fertipaq BV, the Netherlands) with >99% purity (<1% cell material) and 11% moisture content (after dewatering with a centrifuge and sequential drying on a drying cylinder), originating from the Thiopaq process (Paques BV, The Netherlands), was provided at a mass S/N ratio of 3.76 (g/g) (i.e. 1.5 times higher than by stoichiometry in Eq. (1) (Mora et al., 2015)) to ensure an adequate concentration of biogenic S^0 for complete NO_3^--N removal, as described previously (Kostrytsia et al., 2018c). The calculation of the theoretical SO_4^{2-} production was done using the stochiometric reactions for two-step denitrification with biosulfur (Eq. (1) and Eq. (2)).

$$S^0 + 0.876\,NO_{3^-} + 0.343\,H_2O + 0.379\,HCO_{3^-} + 0.023\,CO_2 + 0.080\,NH_4^+ \rightarrow 0.080\,C_5H_7O_2N + 0.824\,H^+ + 0.44\,N_2 + SO_4^{2-} \quad \text{(Eq. 1)}$$

$$S^0 + 1.78\,NO_{2^-} + 0.021\,H_2O + 0.158\,HCO_{3^-} + 0.010\,CO_2 + 0.034\,NH_4^+ \rightarrow 0.034\,C_5H_7O_2N + 0.099\,H^+ + 0.888\,N_2 + SO_4^{2-} \quad \text{(Eq. 2)}$$

2.3. Experimental design

2.3.1. Carrier colonization phase: fed-batch MBBR operation

The four MBBRs were operated parallelly in fed-batch mode to enrich the biogenic S^0-based denitrifying bacterial cultures and allow the microorganisms colonize the carriers prior to starting the continuous-flow operation. The enrichment was considered 'stable' after 6 months when the nitrate removal rate varied by less than 5% between subcultures in MBBRs. The reactors were filled with the mineral medium and trace element solution, and half of the MBBR volume was replaced with a fresh feed solution when the NO_3^--N concentration approached zero. The pH was adjusted to 8.5 by the addition of 5 N NaOH.

2.3.2. Experimental conditions during continuous-flow MBBR operation

After the 6-month enrichment phase, the four MBBRs were operated in parallel in continuous mode for 309 days to investigate the effects of HRT, biofilm carrier type (K1 and Z-200) and biogenic S^0 dosage on denitrification by ADBIOS (Table 1). For the first 92 days, the biogenic S^0 was dosed daily, in the form of powder, to the MBBRs and HRTs of 72, 48, 36 and 24 h were tested. Between days 92 and 206, the four MBBRs were operated at HRTs of 36, 30 and 24 h (Table 1), and biogenic S^0 was continuously supplied as a suspension from a separate feed canister. After day 206, the HRT was gradually decreased from 48 to 21 h and biogenic S^0 was supplied twice a day in the form of powder directly into the MBBRs.

2.4. Sampling and analytical techniques

Effluent samples were taken every second day from a sampling port located before the effluent tank (Figure S1). Anion concentrations (NO_2^-, NO_3^-, SO_3^{2-}, SO_4^{2-} and $S_2O_3^{2-}$) were analyzed by ion chromatography as reported elsewhere (Kiskira et al., 2017). Elemental S^0 concentrations were measured by reversed-phase chromatography as reported by Kostrytsia et al. (2018c) and Kamyshny et al. (2009). The sulfide (S^{2-}) concentration was analyzed spectrophotometrically (Cord-Ruwisch, 1985). The pH, temperature, DO and ORP were measured by a pH sensor (HI11312 HALO, Hanna Instruments, USA), DO portable meter (ProfiLine Oxi 3205, WTW, Germany) and ORP electrode (SenTix® ORP, WTW, Germany), respectively.

The mature biofilm carriers (10 of K1 and 7 of Z-200, respectively) were sampled directly from each MBBR (Figure S1) at the end of each experimental condition (Table 1), replaced with the new carriers and stored at −80 °C prior to analysis. The mass of the biofilms developed onto the carrier material, represented as attached TS (g $TS_{attached}$), was quantified as previously described (Piculell et al., 2016). In this study, the concentration of mass of the biofilm was expressed as attached biomass concentration (g $TS_{attached}$/L).

2.5. Microbial community analysis

2.5.1. DNA and RNA co-extraction, and high-throughput sequencing

Total genomic DNA and RNA was co-extracted from biofilm (K1 for MBBR1 and MBBR2; and Z-200 for MBBR3 and MBBR4) at seven different time points (days 0, 63, 77, 144, 206, 223 and 264) according to the protocol by Griffiths et al. (2000). The concentrations of extracted DNA and RNA were measured spectrophotometrically (UV–Vis spectrophotometer, NanoDrop Technologies, Wilmington, USA). DNA and RNA were kept at −20 °C and −80 °C, respectively, prior to further analyses.

The RNA extracts were exposed to DNase treatment using a TURBO DNase-*free*™ Kit (Thermo Fisher Scientific, Lithuania) for the removal of residual DNA. Bacterial 16S rRNA genes were amplified by polymerase chain reaction (PCR) using primers 515F and 806R. To confirm the efficiency of DNA removal, the PCR products were visualized on 1% agarose gel electrophoresis. Subsequently, the synthesis of first-strand cDNA was performed using SuperScript™ IV First-Strand Synthesis System (Thermo Fisher Scientific, Lithuania). Finally, the quality of the cDNA and DNA was confirmed using electrophoresis and PCR. The 16S rRNA gene amplicons derived from the DNA and cDNA samples were sequenced using an Illumina MiSeq platform (FISABIO, Spain). Raw sequence files supporting the results of this article are available in the European Nucleotide Archive under the project accession number PRJEB45924 with sample information available (Supplementary Table S1).

2.5.2. Bioinformatics and statistical analysis

Bioinformatics and statistical analysis are described in the supplementary material (Supplementary file 1).

Table 1
Experimental continuous-flow conditions of the MBBRs operated at 30 (±2) °C for ADBIOS of a synthetic wastewater containing 225 mg NO_3^--N/L and biogenic S^0 as electron donor at an S/N (g/g) ratio of 3.76.

Time (days)	0–50	50–63	63–77	77–92	92–144	144–166	166–206	206–223	223–247	247–264	264–280	280–309
HRT (h)	72	48	36	24	36	30	24	48	36	30	24	21
Nitrogen loading rate (NLR) (mg NO_3^--N/L·d)	75.0	112.5	150.0	225.0	150.0	180.0	225.0	112.5	150.0	180.0	225.0	257.1
Sulfur loading rate (SLR) (mg S^0/L·d)	282.0	423.0	564.0	846.0	564.0	676.8	846.0	423.0	564.0	676.8	846.0	966.7
S^0 supply	Powder (dosed once a day)				Pumped in suspension from a feed canister				Powder (dosed twice a day)			

3. Results and discussion

3.1. Colonization of carriers by the S^0-oxidizing denitrifying population

ADBIOS was initially maintained in duplicate MBBRs filled respectively with K1 and Z-200 biofilm carriers with fed-batch operation (Section 2.3.1). The nitrate removal rate increased from 30.1 (±2.5) to 73.0 (±12.0) mg NO_3^--N/L·d, whereas NO_2^--N accumulation varied between 0 and 85.7 (±10.7) mg/L during the enrichment phase (data not shown). The DO was equal to 0.5 (±0.1) mg/L, which is slightly above the maximum level of 0.5 mg/L for effective autotrophic denitrification (Christianson et al., 2015; Wang et al., 2016). The temperature was maintained at 30.4 (±0.3) °C, which is within the optimal range of 30–35 °C (Kostrytsia et al., 2018a). At the end of the 6-month enrichment (Section 2.3.1), a microbial community capable of simultaneous NO_3^--N removal and biogenic S^0 oxidation to SO_4^{2-}S colonized the biofilm carriers (Section 3.4.2), resulting in an attached concentration of 0.14 (±0.07) and 0.020 (±0.005) g $TS_{attached}$/L (data not shown) in the MBBRs with the K1 and Z-200 biofilm carriers, respectively.

3.2. ADBIOS performance with the two different biofilm carriers under increasing nitrate loading rate

The ADBIOS performance in the MBBRs operated with the two different biofilm carriers was compared by increasing the nitrogen loading rate (NLR) from 75.0 to 257.1 mg NO_3^--N/L·d (Fig. 1).

3.2.1. Days 0–92: biosulfur supplied daily in the form of powder

During the first 92 days, the HRT was gradually reduced from 72 to 24 h and biosulfur was supplied daily in the form of powder at an S/N (g/g) ratio of 3.76 (Table 1). During the first 29 days of continuous MBBR operation, the effluent NO_3^--N concentration fluctuated between 50 and 200 mg/L, as similarly reported for other S^0-based denitrification studies (Sahinkaya et al., 2014; Wang et al., 2016) At an HRT of 72, 48 and 36 h, a complete denitrification was achieved with the effluent SO_4^{2-}S concentration remaining stable at approximately 580 mg/L in all MBBRs and was similar to the theoretical value for complete NO_3^--N degradation, according to the stoichiometry proposed by Mora et al. (2015) (Fig. 1d). However, when further decreasing the HRT to 24 h (day 77–91), the NO_3^--N removal efficiency dropped to 58 (±7)% and resulted in a NO_2^--N accumulation of 96 (±20) mg/L and a reduced SO_4^{2-}S production (Fig. 1a–b, d, day 84–91) was observed. Decreasing the HRT to 24 h promoted a quick wash-out of the biosulfur that was confirmed by the reduced S^0 concentrations in the effluents to 55 (±20) mg/L (Fig. 1c), and bacteria were thus exposed to lower S^0 concentrations of than those stoichiometrically required for complete denitrification. Until day 92, NO_3^--N removal resulted in acidity production with the pH dropping from 8.5 to 6.9 (±0.3) in the MBBR effluents (Figure S3a), which corresponds to what was observed in a previous study on S^0-fueled denitrification (Sahinkaya et al., 2015). The ORP in the MBBRs was between −63 (±7) and +16 (±8) mV on average, and DO concentrations remained below 0.07 mg/L (Figure S3).

3.2.2. Days 92–206: continuous supply of S^0 as a suspension

On day 92, the HRT was increased up to 36 h to recover the system from the unstable operation in the previous phase (Fig. 1a and b, day 77–91). Simultaneously, the biosulfur dosage strategy was changed to a continuous supply of S^0 as a suspension from a feed tank at an S/N (g/g) ratio of 3.76 to continuously provide, and retain, sufficient electron donor in the denitrifying MBBRs. At the 36-h HRT, effluent NO_3^--N concentrations decreased, and varied between 31 and 65 mg/L (Fig. 1a, day 92–130), whilst the accumulated NO_2^--N fluctuated between 60 and 147 mg/L (Fig. 1b, day 92–130), resulting in a higher SO_4^{2-}S production of up to 448 (±176) mg/L (Fig. 1d, day 92–130).

From day 130–144, a stable MBBR operation was reached with NO_3^--N removal efficiencies of 84 (±6)%, NO_2^--N accumulation up to 52 (±14) mg/L and a SO_4^{2-}S production of 593 (±7) mg/L. Further decreasing the HRT to 30 and 24 h (i.e. increasing the NLR to 180.0 and 225.0 mg NO_3^--N/L·d) resulted in NO_2^--N build-up to 128 (±3) mg/L from day 144–151 (Fig. 1b). Subsequently, complete NO_3^- removal occurred between days 152 and 166 (Fig. 1a), likely due to a lower inhibition of denitrifiers at lower NO_2^--N concentrations (below 60 mg/L) (Wang et al., 2016).

At the 24-h HRT (day 166–194), NO_3^--N removal efficiencies in the MBBRs varied between 62 and 100% (Fig. 1a) with a NO_2^--N accumulation up to 169 (±3) mg/L (Fig. 1b) and the SO_4^{2-}S production fluctuated between 163 (±3) and 411 (±28) mg/L. On days 194–206, relatively stable effluent concentrations of 33 (±9) mg NO_3^--N/L, 140 (±3) mg NO_2^--N/L and 274 mg SO_4^{2-}S/L were achieved in the MBBRs. Despite reaching a nitrate removal efficiency of 85 (±5)%, NO_2^--N concentrations above 60 mg/L were observed. NO_2^--N accumulation could most likely be ascribed to an elevated *Nar* activity compared to the nitrite reductase (*Nir*) activity, as similarly reported previously (Wang et al., 2016) and confirmed by microbial analysis in Section 3.4.2.

A continuous supply of S^0 as a suspension (days 92–206) from a feed tank resulted in lower NO_3^--N removal and SO_4^{2-}S production as well as a higher NO_2^--N accumulation (Fig. 1a–b, d). This was explained by a lower S/N ratio than the stoichiometrically predicted one since the

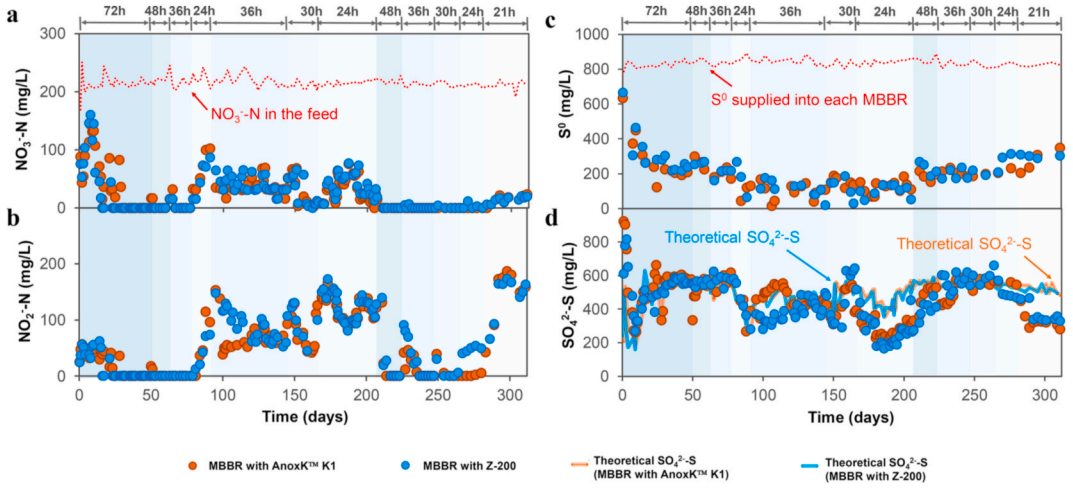

Fig. 1. Performance of the MBBRs performing ADBIOS: **(a)** NO_3^--N concentrations in the effluents and feed; **(b)** effluent NO_2^--N concentrations; **(c)** S^0 concentrations supplied to each MBBR and S^0 concentrations in the effluents; and **(d)** SO_4^{2-}S concentrations in the effluents and the theoretical SO_4^{2-}S productions. The average values of the MBBRs with K1 (MBBR1 and MBBR2) and Z-200 (MBBR3 and MBBR4) supports are plotted.

supplementation of biosulfur in suspension through peristaltic pumps led to clogging of the tubing. Thus, an intermittent supply of sulfur due to tube clogging resulted in either no or insufficient amount of sulfur effectively reached the reactors to support denitrification. This was confirmed by reduced S^0 concentrations in the effluents in a range of 0–190 mg/L (Fig. 1c). At the 24-h HRT (days 166–206), the effluent SO_4^{2-}S concentration was similar to the theoretical value for denitrification, except day for the 170 to 206 period, when its value was up to 35% lower than that suggested by stoichiometry (Fig. 1c–d). This discrepancy might be attributed to either the heterotrophic denitrifiers being active in the environment with an insufficient amount of sulfur for autotrophic denitrification or sulfate-reducing microorganisms using organics from bacterial lysis as electron donor (Section 3.4.2) (Kostrytsia et al., 2018a).

During the experimental phase when biosulfur was dosed continuously as a suspension (days 92–206) (Table 1), the instability of ADBIOS was also reflected by the noticeable fluctuations of the environmental parameters measured in the MBBR effluents. In particular, the effluent pH varied between 6.5 (±0.2) and 7.8 (±0.1) (Figure S3a). DO concentrations increased to 0.34 mg/L (Figure S3c), and the ORP was between −124 (±8) and +42 (±3) mV (Figure S3b), which is in the optimal ORP range of −100 to +50 mV for S^0-driven denitrification (Sahinkaya et al., 2015).

3.2.3. Days 206–309: biosulfur supplied twice a day in the form of powder

To discount kinetic limitation of the denitrifying community and guarantee an enough amount of biosulfur, an HRT of 48 h was used again on day 206 and biosulfur was supplemented in the form of powder (at an S/N (g/g) ratio of 3.76 twice daily as powder directly to the MBBRs). A complete NO_3^--N degradation was rapidly obtained. Subsequently, a stepwise HRT reduction from 48 (day 206–223) to 36 (day 223–247) and 30 h (day 247–264) also resulted in complete NO_3^--N and NO_2^--N removal (Fig. 1a-b), except for a few NO_2^--N peaks at the beginning of each operational phase, i.e. on days 212–214, 226–235, and 249. Simultaneously, SO_4^{2-}S production (Fig. 1d) was in accordance with the stoichiometry proposed by Mora et al. (2015).

At an HRT of 24 h (day 264–309), complete NO_3^--N and NO_2^--N removal was achieved in the MBBRs with K1 (Fig. 1a-b). However, despite a 100% NO_3^--N removal efficiency by the MBBRs with Z-200, a NO_2^--N accumulation up to 54 mg/L (Fig. 1b) resulted a slightly lower SO_4^{2-}S production relative to the stoichiometry (Fig. 1d). The denitrification potential was considerably enhanced by supplementing biosulfur in the form of powder and increasing the S^0 dosage frequency. Therefore, such twice-daily, direct biosulfur dosage allowed for sufficient biogenic S^0 for denitrifiers (Fig. 1c) and a complete NO_3^--N removal with longer and more stable MBBR operation was achieved. Thus, the S/N ratio was shown to be the main factor controlling NO_2^--N accumulation as also previously observed for chemically synthesized S^0-driven autotrophic denitrification (Kostrytsia et al., 2018b). On days 280–309 (at an HRT of 21 h), all MBBRs achieved NO_3^--N removal efficiencies of 90 (±2)% (Fig. 1a) with significant NO_2^--N accumulation up to 180 (±7) mg/L (Fig. 1b) with consequentially lower biosulfur oxidation and reduced SO_4^{2-}S production up to 309 (±25) mg/L (Fig. 1d). Elevated NO_2^--N concentrations are most likely due to a higher *Nar* activity compared to the *Nir* activity, as reported previously (Wang et al., 2016). From day 206 onwards, the effluent pH was equal to 6.6 (±0.3) (Figure S3a), the ORP fluctuated between −138 (±9) and −7 (±4) mV (Figure S3b), and the DO was maintained below 0.1 mg/L (Figure S3c) in all MBBRs.

3.3. Carrier type influences the biomass and sulfur retained in the biofilm

To examine the overall performance of the ADBIOS process in the MBBRs, the evolution of the mass retained in the biofilm and attached onto the K1 and Z-200 carriers was evaluated (Fig. 2). The mass concentration of biofilm onto the Z-200 carriers reached a 4.8 times lower

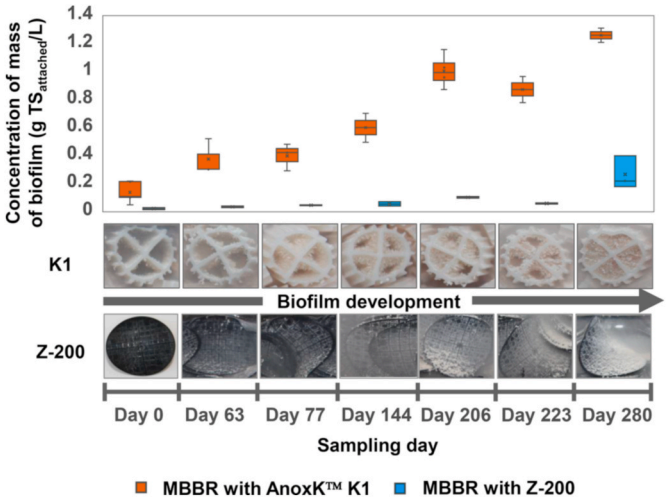

Fig. 2. Concentration (g $TS_{attached}$/L) of mass of biofilm attached onto the K1 and Z-200 carriers used in MBBR1-MBBR2 and MBBR3-MBBR4, respectively, and photographs of representative carriers sampled on days 0, 63, 77, 144, 206, 223 and 280.

final value, i.e. 0.26 (±0.11) g $TS_{attached}$/L, compared to that for K1 carriers (Fig. 2). This is likely attributed to the pre-defined grid height of the Z-200 carrier, which determines a maximum biofilm thickness of 200 μm, and the open design resulting in higher internal fluid velocity and induced shear (Piculell et al., 2016). In contrast, K1 carriers (with 10-mm diameter and 7-mm length) do not have such a pre-defined limit for biofilm thickness and are also less exposed to shear (Ødegaard et al., 1994). To investigate the effect of the hydrodynamic behavior on the working performance of the reactor in more detail, a tracer study and numerical simulations are recommended for future research, as similarly done by Wang et al. (2021).

Nonetheless, despite having a significantly lower mass of biofilm (Fig. 2), the MBBRs with Z-200 carriers supported similar nitrate removal rates to those achieved in the MBBRs with K1 carriers (Section 3.2). This is likely attributed to the microbial communities being similar on both the K1 and Z-200 carriers (Procrustes analysis and Mantel test in Section 3.4.1 and Table S2). Simultaneously, the MBBRs operated with the classical K1 carriers tolerated better HRTs lower than 30 h, as also indicated by the lower NO_2^--N accumulation compared to the Z-200 MBBR. This could be explained by a relatively stable microbial community being formed in the MBBRs with K1 carriers over time in contrast with the MBBRs with Z-200 carriers (Section 3.4.2 and Fig. 5).

A significant inactive or inert fraction was present in the biofilm grown on the K1 carrier during the entire MBBR operation and part of the supplemented biogenic S^0 was retained in the biofilm (Fig. 3a). Freeze-drying of samples of the biofilm attached onto the carriers prior to scanning electron microscopy (SEM) and Raman spectroscopic analysis is known to crystalize biosulfur (Kamyshny et al., 2009). Thus, SEM images show that the surface of the microbial cells in the biofilm was covered with crystals (indicated by the star in Fig. 3). EDS spectra showed a relative atomic percentage of approximately 15.2 (±1.8)% and 9.5 (±0.7)% for sulfur (S) onto K1 and Z-200 carriers, respectively. In addition, the biofilms on both carriers contained 75 (±8)% carbon (C), 10 (±5)% oxygen (O), and less than 1% chlorine (Cl) and calcium (Ca). Raman spectra of biogenic S^0 inclusions showed no peaks other than those of elemental sulfur with a ring configuration and orthorhombic (S_8) crystalline structure (Fig. 3). S_8 is the most thermodynamically stable form of S^0 and is typically formed at neutral pH (Meyer, 1976), which was maintained inside the MBBRs in this study (Figure S1a). This is in accordance with Guo et al. (2019), who confirmed that nearly all the reduced sulfur was stored as S^0 inclusions in the sludge of a sequencing batch reactor (SBR) used for sulfur-driven

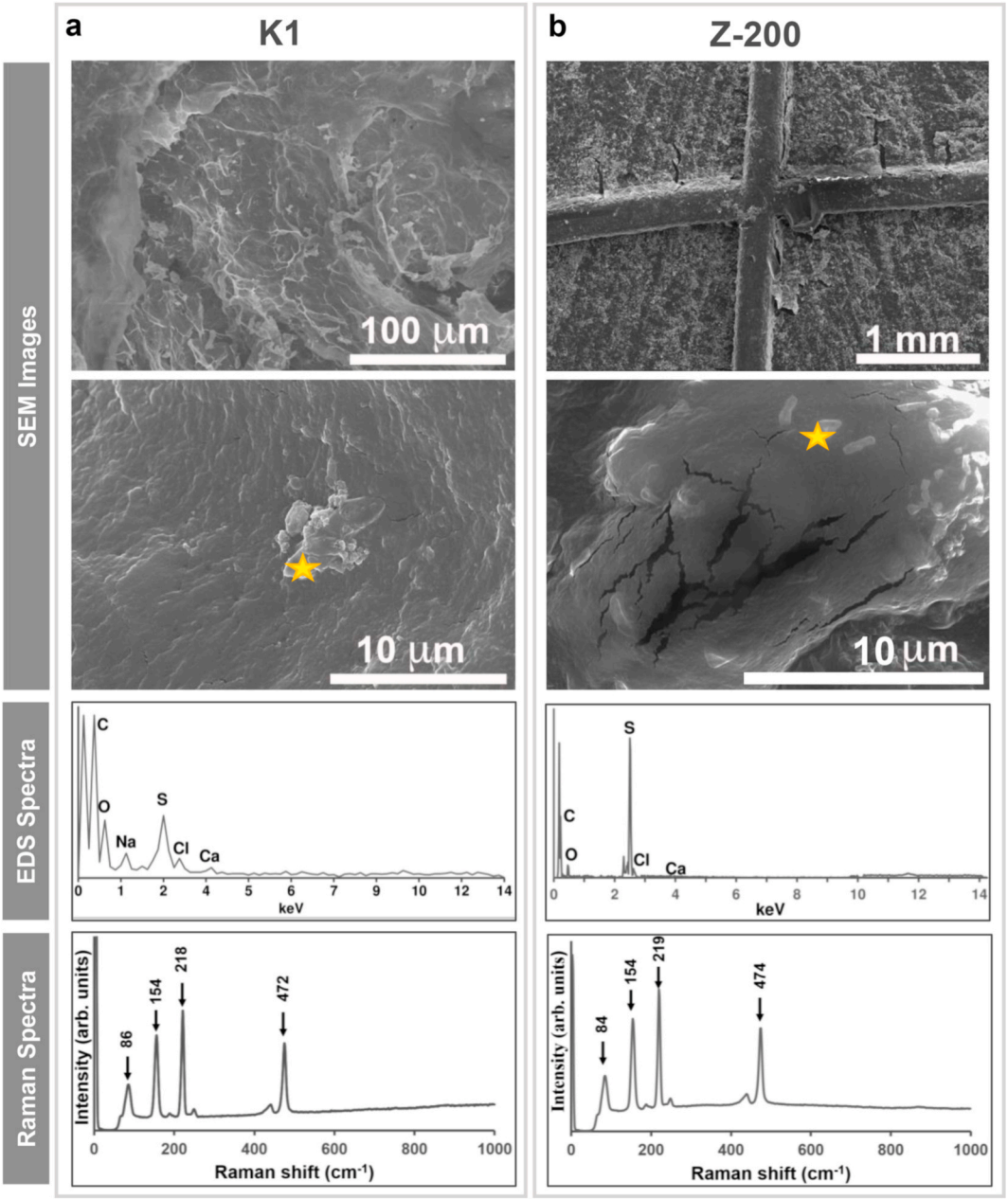

Fig. 3. SEM micrograph, EDS and Raman spectra of the biofilm growing on the **(a)** K1 and **(b)** Z-200 carriers sampled on day 280 from MBBRs. Stars indicate the points where EDS spectra were obtained.

denitrification and phosphorus removal of a synthetic saline wastewater. However, the microbiological analysis (Section 3.4.2) did not show the presence of bacteria belonging to the *Helicobacteraceae* family, which were suggested previously to be the hydrolytic biomass capable of solubilization chemically-synthesized S^0 (almost water insoluble) for denitrification (Kostrytsia et al., 2018a). Therefore, in studies on biosulfur-driven denitrification in both MBBRs (this study) and batch microcosms (Kostrytsia et al., 2018c), the absence of bacteria belonging to the *Helicobacteraceae* family was observed, suggesting a direct bioavailability of biosulfur for the denitrifying bacteria in the MBBRs.

3.4. Carrier type affects the diversity, structure and activity of the microbial community

3.4.1. Diversity of the bacterial communities

The difference within (alpha diversity) and between (beta diversity) each microbial community, as well as the effect of environmental processes (environmental filtering) on selected microbial communities, is shown in Fig. 4. The richness (Alpha diversity) of the active portion of the microbial community (cDNA-based OTUs) was lower than for the total community (DNA-based OTUs) in both biofilms growing on the K1 and Z-200 carriers. In addition, the active community members had very high the nearest taxa (NTI) to net relatedness index (NRI) (much higher than 2), indicating a clustered phylogeny, imply a strong influence of environmental pressure. This was further confirmed by observing the cDNA-based microbial communities clustered closely on PCoA plots (unweighted Unifrac plot, Fig. 4).

Despite having little commonality in terms of abundance of dominant taxa (Bray-Curtis PCoA plot), the active microbial communities shared similarity in terms of phylogeny within each carrier type (unweighted Unifrac PCoA plot) (Fig. 4). Phylogeny had more impact than abundance for microbial communities of each carrier type

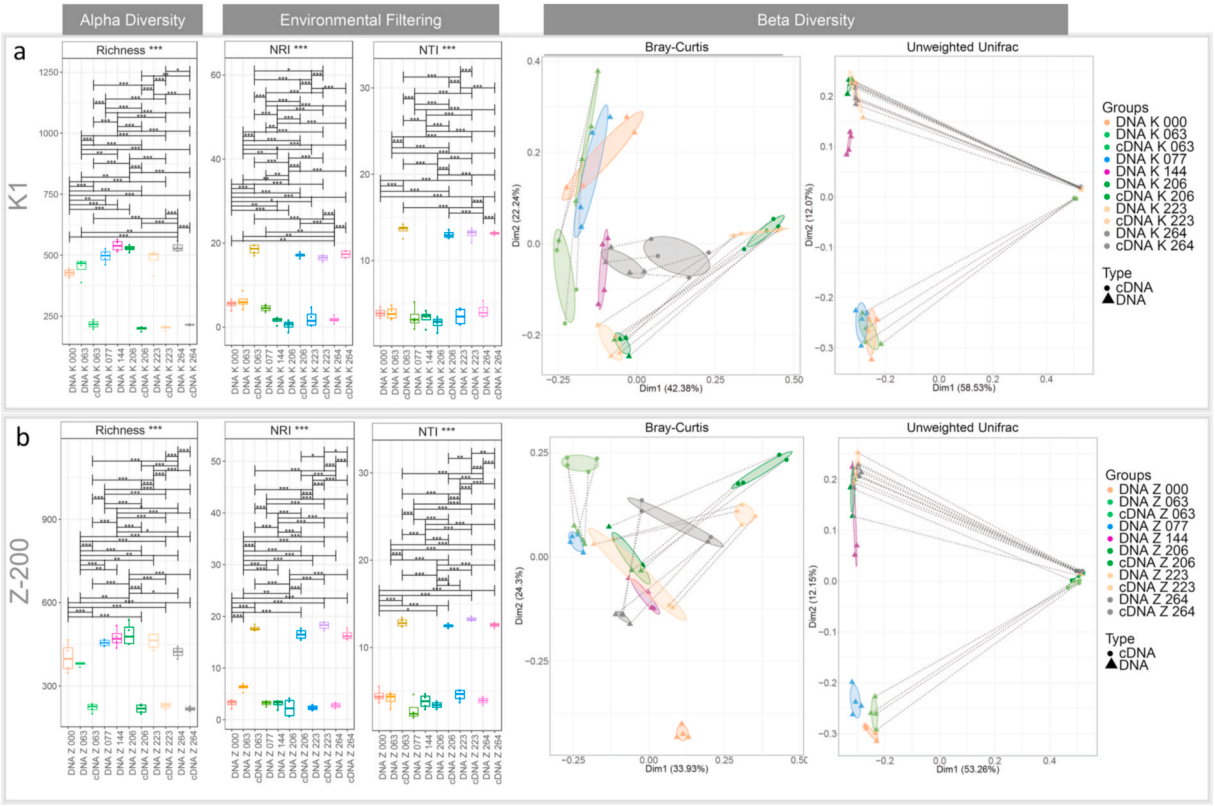

Fig. 4. Diversity measures for **a)** K1 (K) and **b)** Z-200 (Z) carriers using both DNA and cDNA samples colored according to the day of MBBR operation. For environmental filtering, stochastic and deterministic nature of communities using NRI and NTI were investigated. For Principal Coordinate Analysis (PCoA), ellipses represent 95% confidence interval of the standard errors, and where the DNA and cDNA profiles come from the same samples, points are connected with dotted lines.

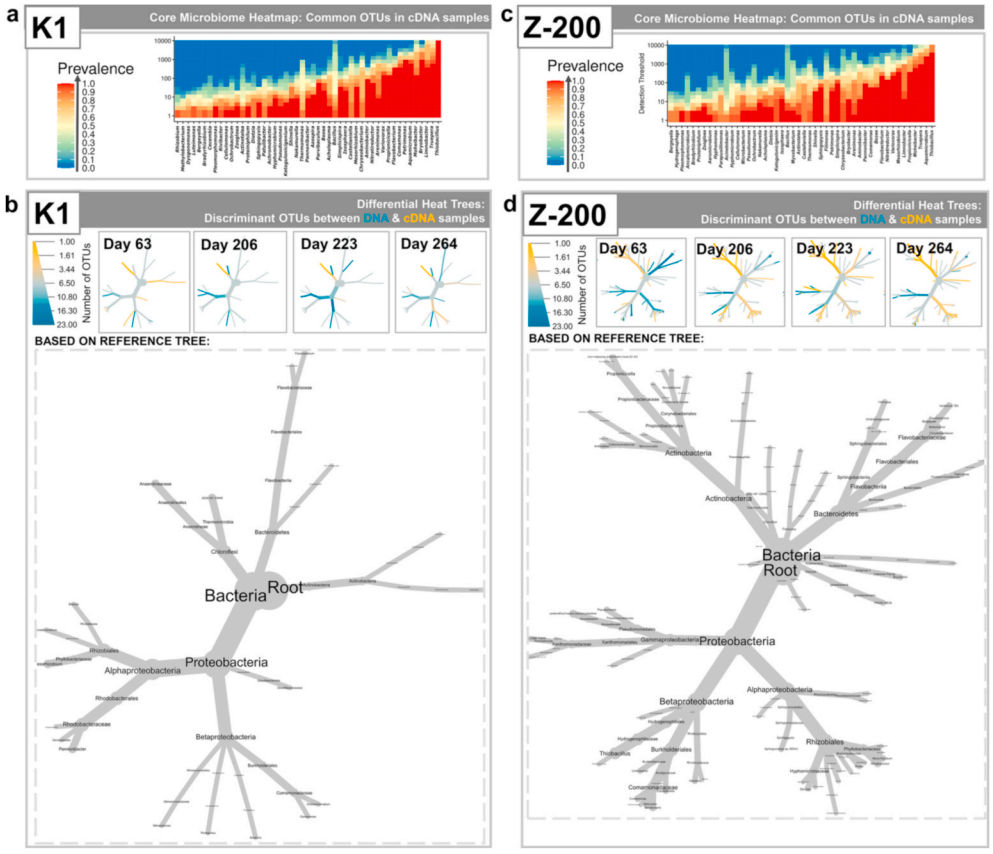

Fig. 5. The comparison of the microbial communities between those being present (DNA-based) and active (cDNA-based) for each type of biofilm carrier (K1 and Z-200) in order to evaluate the stability of microbial community overtime. **(a)** and **(c)** are heatmaps showing the core cDNA microbiome at a minimum of 85% prevalence for biofilms onto K1 and Z-200 carriers, respectively; and **(b)** and **(d)** show the references tree (grey) and the differential heat trees with the colored branch representing the dominant OTUs either in the DNA or cDNA samples taken at the known day of MBBRs operation.

(Environmental Filtering plot) (Fig. 4). Therefore, in view of the environmental filtering (NRI/NTI) and PCoA (unweighted Unifrac) results, it is likely that specific clades were selected. In addition, the Procrustes analysis illustrated that at DNA level both K1 and Z-200 biofilms have a very high correlation ($R = 0.981$ with $p = 0.001$) in terms of phylogeny (unweighted Unifrac). This means that at DNA level the same species were present on both the K and Z carriers, although they differed in abundance (lower correlation in terms of Bray-Curtis distance) (Table S2). Hence, at DNA level the microbial communities followed the same trend for the K1 and Z-200 MBBRs and could be considered similar (Mantel test). However, at the cDNA level K1 and Z-200 biofilms demonstrate temporal similarity only in terms of abundance ($R = 0.953$ with $p = 0.042$) (Table S2).

3.4.2. Microbial community structure and activity

The core microbiome (DNA-based), where genera persisted in 85% of the samples for the K1 and Z-200 carriers, included *Thiobacillus*, *Moheibacter*, *Truepera* and *Arenimonas* at the DNA level (Figure S4), suggesting that these bacterial groups play an important role in the ADBIOS process. Other genera comprising the core microbiome were identified at varying abundances within K1 and Z-200 biofilms (Figure S4). However, at cDNA level the abundance of *Arenimonas* was significantly lower for both types of carriers. Instead, *Bryobacter* and *Limnobacter* for K1 carrier, and *Aquamicrobium* and *Propionicicella* for Z-200 carriers, characterised the core microbiome. *Thiobacillus* (based on DNA studies) is usually detected as a dominant group in sulfur-based autotrophic denitrification (Kostrytsia et al., 2018c; Wang et al., 2016). *Truepera* and *Moheibacter* (affiliated with the family *Xanthomonadaceae*) were detected in previous ADBIOS batch experiments using the same inoculum sludge as in this study (Kostrytsia et al., 2018a). Microorganisms belonging to *Truepera* possess *Nar*, *Nir*, nitric oxide reductase (*Nor*) (KEGG PATHWAY: tts00910) and sulfur oxidizing (*Sox*) (KEGG PATHWAY: tts00920) enzymes. The presence of the *Moheibacter* genus was positively correlated with NO_3^-, but not NO_2^- degradation (Kostrytsia et al., 2018c). Bacteria within the *Arenimonas* genus (belonging to family *Xanthomonadaceae*) have been enriched previously in denitrification bioreactors (Wang et al., 2020). Bacteria within the *Propionicicella* taxa can use both NO_3^- and NO_2^- to perform heterotrophic denitrification (Kostrytsia et al., 2018a). Species related to denitrification within the *Aquamicrobium* genus have previously been enriched in the anoxic denitrification systems (Wang et al., 2020).

Within the core microbiome of the K1 biofilm, the same genera were abundant in both DNA and cDNA samples, implying that most of the microorganisms present within biofilms (Figure S4) were those performing metabolic activities (based on cDNA data) (Fig. 5b). In addition, a relatively stable microbial community was formed in MBBR1 and MBBR2 (Figure S4). The K1 carrier is designed to develop biofilm in the inner part of the cylindrical-shape carrier, which is not subjected to direct collision with other carriers and, thus, protected from hydraulic shear. This likely helped MBBRs with the K1 carrier to develop a thick biofilm with a relatively stable microbial community over time. Furthermore, this may be associated with the better performance of MBBR with K1 compared to that of MBBR with Z-200 (Section 3.2).

In contrast, distinct genera, including *Propionicicella*, *Variovorax* and *Bosea*, were shown to be active in Z-200 biofilm (Fig. 5) though less abundant (Figure S4). Bacteria within the *Bosea* genus are capable of NO_3^- reduction coupled to the *Sox* pathway (KEGG PATHWAYs: bos00920, deq00920 and ctt00920; Wang et al., 2020). The bacteria belonging to the *Variovorax* genus have been reported in previous S^0-based denitrification studies (Gao et al., 2017; Hao et al., 2017). Moreover, the microbial community varied significantly over time in MBBRs with Z-200 carriers (Fig. 5). This is likely caused by the novel AnoxK™ Z-carrier being designed to allow the biofilm to grow only on the carrier surface, but in a protected environment thanks to the presence of a grid of defined height. However, due to scouring from other carriers (abrasion), such biofilm cannot grow higher than the grid height, and so biofilm thickness is controlled. The diffusion of the soluble substrates (nitrate, biosulfur and nitrite) would be easier through the thin Z-200 biofilm, in contrast to the thicker biofilm developed onto K1 carriers. But, the presence of a thinner biofilm results under varying operating conditions led to a more frequent turnover of the species colonizing the biofilm, as revealed by the significant variation over time of the active microbial community (cDNA-based) in MBBRs with Z-200 carrier.

Thermomonas and *Pseudomonas* (affiliated with family *Xanthomonadaceae*), *Opitutus, Nitratireductor and Variovorax* genera were abundant on days 144 and 206 and rarer on other sampling days, on K1 and Z-200 biofilms (Figure S4a), and were associated with process failure: significant NO_2^--N accumulation (above 60 mg/L, see Section 3.2) resulting in reduced NO_3^--N removal rates (Fig. 1a). These genera were also a part of the core microbiome, and were more abundant in the K1 versus Z-200 biofilm. Microorganisms belonging to the *Xanthomonadaceae* family are capable of NO_3^- and NO_2^- respiration using organic products from cell lysis as electron donors (Xu et al., 2015). In addition, bacteria within the *Thermomonas* genus were predominately selected by NO_2^--N (up to 240 mg/L) reduction with biogenic S^0 (Kostrytsia et al., 2018c). Bacteria within the *Opitutus* genus possess the complete set of genes encoding both denitrification and ammonification pathways (Espenberg et al., 2018). The bacteria belonging to the *Nitratireductor* genera are capable to degrade both NO_3^- and NO_2^- and were detected previously in ADBIOS batch experiments (Kostrytsia et al., 2018a). Microorganisms belonging to *Variovorax* possess *Nar* and *Nor* (KEGG PATHWAY: vpd00910) and *Sox* (KEGG PATHWAY: tts00920) enzymes.

The active members (cDNA-based analysis) of the microbial community that were relatively more abundant on day 206, comparison with day 63, were also associated with process failure: significant NO_2^--N accumulation (above 60 mg/L, see Section 3.2) resulting in reduced NO_3^--N removal rates (Fig. 1a). Only three bacterial taxa were identified as upregulated in the cDNA (higher in the cDNA than in DNA) on day 206 in the K1 MBBR (Fig. 5), including *Desulfobacteraceae*, *Flavobacteriaceae* and *Anaerolineaceae*. *Desulfobacteraceae* are capable of SO_4^{2-} reduction (KEGG PATHWAYs: dat00920). Microorganisms belonging to the *Flavobacterium* genus, being a part of the core cDNA -based microbiome of the K1 biofilm in this study, are capable of heterotrophic denitrification (Drysdale et al., 1999) and have *Nir* and *Nor* enzymes (KEGG PATHWAY: fjo00910). The bacteria belonging to *Anaerolineaceae* taxa possess the *Nir* enzyme (KEGG PATHWAY: tro00910).

In contrast, eight taxonomical groups were identified as upregulated on day 206 in comparison to day 63 (Fig. 5) for MBBRs filled with Z-200, including a few genera belonging to *Alphaproteobacteria* (*Ochrobactum*, *Shinella*, *Bosea*, *Aquamicrobium*, *Aminobacter* and *Nitratireductor*), the *Limnobacter* genus and the *Ignavibacteriaceae* family. The above-mentioned taxa are part of the core microbiome (cDNA-based) of the Z-200 biofilm and convert both NO_3^- and NO_2^- to N_2. *Limnobacter*, *Shinella* and *Aminobacter* were detected in reactors supplied with reduced sulfur compounds (including biosulfur) treating NO_3^- and NO_2^- pollution (Christianson et al., 2015; Kostrytsia et al., 2018c). *Ignavibacteriaceae* have recently been identified as associated with S^0-based autotrophic denitrifying processes and tolerated NO_2^--N concentrations up to 240 mg/L (Kostrytsia et al., 2018a). Some denitrifying bacteria within the *Ochrobactum* genus have evolved NO_2^- tolerance mechanisms and can degrade up to 1800 mg/L NO_2^--N (Doi et al., 2009). Therefore, based on cDNA samples, different microbial groups were associated with process failure for K1 and Z-200 biofilms. This is likely explained by easier diffusion of the soluble substrate like NO_2^- through the thin Z-200 biofilm, in contrast to the thicker biofilm developed onto K1 carriers.

3.5. Engineering significance of ADBIOS in MBBRs

ADBIOS could be effectively maintained (i.e. NO_3^--N completely

removed without NO_2^- accumulation) in MBBRs operated at an HRT as low as 24 and 30 h with K1 and Z-200 carriers, respectively. Under those conditions, the highest nitrate removal rates were approximately 225 (±11) mg/L and 180 (±7) mg NO_3^--N/L·d in the MBBRs operated with K1 and Z-200 carriers, respectively. These values were 10.7 and 8.6 times higher for K1 and Z-200 biofilm carriers, respectively, compared to the highest NO_3^--N removal rate of 20.9 mg/L·d obtained in batch experiments using suspended biomass (Kostrytsia et al., 2018c).

High removal rates were also promoted by the hydrophilic properties and smaller particle size of biosulfur (Findlay et al., 2014) as well as the MBBR characteristics, which enhance the contact between substrates and microorganisms compared to other treatment systems used for S^0-based autotrophic denitrification (Lemaire et al., 2013).

Similarly, studies on autotrophic denitrification with chemically synthesized S^0 in packed-bed reactors (PBR) achieved nitrate removal rates of 100–400 mg/L·d at HRTs of 0.5–26 h (Simard et al., 2015; Ucar et al., 2020), typically with incomplete NO_3^- removal. In addition, the high concentrations of S^0 in such non-thoroughly mixed systems as PBRs increased S^{2-} production as a result of S^0 disproportionation or SO_4^{2-} reduction (Sierra-Alvarez et al., 2007). S^{2-} is an environmental and industrial pollutant because of its toxicological effects even at low concentrations (Sahinkaya et al., 2011). Contrarily, during the ADBIOS process investigated in this study, the influent biosulfur concentration was only 1.5 times higher than the stoichiometric value for complete denitrification (Fig. 1c), and the use of the MBBR technology allowed a complete mixing and homogenously anoxic conditions in the reactors, thus hampering the probability of S^{2-} production. Thus, the S^{2-} concentration in the MBBR effluent was below the detection limit of 0.5 mg/L (data not shown). Besides, throughout the MBBR operation, neither SO_3^{2-} nor $S_2O_3^{2-}$ were detected in the effluent (data not shown).

Higher nitrate removal rates (up to 800 mg NO_3^-N/L·d with HRTs as low as 5 min) were observed in fluidized-bed reactors (FBRs), due to the absence of clogging and a better mass transfer of NO_3^- to the S^0 particles, despite the higher energy demands and physical size for bed fluidization (Christianson et al., 2015). Recently, Ucar et al. (2020) investigated biogenic S^0-oxidizing membrane bioreactors (MBRs) performing autotrophic denitrification of drinking water at HRTs of 6–26 h and reported complete denitrification with a nitrate removal rate of 286 mg NO_3^-N/L·d. Nonetheless, membrane fouling was described as an important drawback of the set-up. Therefore, this study highlights the reliability of the MBBR technology in maintaining ADBIOS, provided that biosulfur is properly dosed and a sufficiently high HRT is used, opening new perspectives for the treatment of nitrate contaminated wastewaters with low C/N ratio.

Based on the results of this study, it is recommended that biosulfur is supplemented periodically in the form of powder. When supplying biosulfur as suspension from a feed canister, an intermittent supply of sulfur due to tube clogging would cause either no or insufficient amount of sulfur effectively dosed to the reactors to support denitrification. An automatic biosulfur dosage would be easy to implement at larger, e.g. industrial scale, systems to supply the required (equal to stochiometric value) quantity of biosulfur to minimize the chances of wash out.

Despite MBBRs with both K1 and Z-200 carriers showed similar NO_3^- removal rates, MBBRs with K1 carriers had lower NO_2^--N accumulation, higher mass of biofilm and developed a relatively stable microbial community over time. The higher shear stress onto the Z-200 carrier due to its open design and direct collision with other carriers resulted in a thinner biofilm being developed onto Z-200 carriers. Therefore, a better diffusion of the soluble substates would be observed onto Z-200 carriers. But, the presence of a thinner biofilm results under varying operating conditions led to a more frequent turnover of the species colonizing the biofilm, as revealed by the significant variation over time of the active microbial community (cDNA-based) in MBBRs with Z-200 carrier.

In contrast, biofilm growth in the inner part of the cylindrical-shape K1 carrier resulted in its protection from hydraulic shear and development of thicker biofilm with partial substrate diffusion. Therefore, any further increase in biofilm thickness would not benefit the ADBIOS process due to 1) reduced biofilm area, 2) potential anaerobic zones causing S^{2-} production by sulfate-reducing bacteria, and 3) increased weight of the carrier (Boltz and Daigger, 2010). Specifically, uncontrolled biofilm growth might be associated with a higher level of inorganic inclusions, including biosulfur, as observed for the K1 biofilm in this study.

4. Conclusions

- Complete denitrification with biogenic S^0 supplied twice a day in the form of powder was achieved in the MBBRs operated with AnoxK™ 1 (K1) and Z-200 carriers at nitrogen loading rate of 225 and 180 mg NO_3^--N/L·d, respectively.
- The MBBRs operated with the classical K1 carriers better tolerated HRTs lower than 30 h, as also indicated by the lower NO_2^--N accumulation observed than in the Z-200 MBBR.
- Despite having the same protected surface area for biofilm development in each MBBR, the mass of biofilm attached onto the K1 carrier reached a 4.8-fold higher value than that on the Z-200 carrier, with part of the biogenic S^0 retained in the biofilm.
- While being similar at DNA level, at cDNA level K1 and Z-200 biofilms demonstrate temporal similarity only in terms of abundance ($R = 0.953$ with $p = 0.042$) with phylogenic distances being not similar.
- A relatively stable microbial community was formed in MBBRs with K1 carrier over time, while the active microbial community (cDNA-based) varied significantly over time in MBBRs with Z-200 carriers
- Based on cDNA samples, more microbial groups were associated with process failure for Z-200 than K1 biofilms, including the *Limnobacter* genus and a few genera belonging to *Alphaproteobacteria* and *Ignavibacteriaceae* families.

Declaration of competing interest

The authors declare that they have no known competing financial interests or personal relationships that could have appeared to influence the work reported in this paper.

Acknowledgements

We thank Gelsomino Monteverde and Manuel Di Ruscio for assisting in reactor operation and Anna Trego for performing the synthesis of the first-strand cDNA. This work was supported by the Marie Skłodowska-Curie European Joint Doctorate (EJD) in Advanced Biological Waste-To Energy Technologies (ABWET) funded by the Horizon 2020 program under the grant agreement no. 643071. The authors acknowledge Fertipaq B.V. (The Netherlands) for providing the biogenic sulfur, and Veolia Water Technologies AnoxKaldnes (Sweden), for supplying the AnoxK™ Z-200 biofilm carriers. G.C. was supported by a Science Foundation Ireland Career Development Award (17/CDA/4658). U.Z.I. was supported by a NERC Independent Research Fellowship (NE/L011956/1) and EPSRC (EP/P029329/1 and EP/V030515/1).

Appendix A. Supplementary data

Supplementary data to this article can be found online at https://doi.org/10.1016/j.chemosphere.2021.131975.

Credit author statement

A. Kostrytsia: Conceptualization, Methodology, Formal analysis, Investigation, Visualization, Writing – original draft, Writing – review & editing. **S. Papirio:** Conceptualization, Methodology, Writing – review & editing. **M. Khodzhaev:** Investigation. **L. Morrison:** Investigation, Resources. **G. Collins:** Resources, Writing – review & editing,

Visualization. **P.N.L. Lens:** Conceptualization, Writing – review & editing. **U.Z Ijaz:** Data Formal analysis, Visualization, Writing – review & editing. **G. Esposito:** Conceptualization, Writing – review & editing, Resources, Supervision, Funding acquisition.

Data availability

The sequencing data are available on the European Nucleotide Archive under the study accession number: PRJEB45924 (http://www.ebi.ac.uk/ena/data/view/PRJEB45924).

References

Bassin, J.P., Dias, I.N., Cao, S.M.S., Senra, E., Laranjeira, Y., Dezotti, M., 2016. Effect of increasing organic loading rates on the performance of moving-bed biofilm reactors filled with different support media: assessing the activity of suspended and attached biomass fractions. Process Saf. Environ. Protect. 100, 131–141. https://doi.org/10.1016/j.psep.2016.01.007.

Boltz, J.P., Daigger, G.T., 2010. Uncertainty in bulk-liquid hydrodynamics and biofilm dynamics creates uncertainties in biofilm reactor design. Water Sci. Technol. 61 (2), 307–316. https://doi.org/10.2166/wst.2010.829.

Christianson, L., Lepine, C., Tsukuda, S., Saito, K., Summerfelt, S., 2015. Nitrate removal effectiveness of fluidized sulfur-based autotrophic denitrification biofilters for recirculating aquaculture systems. Aquacult. Eng. 68, 10–18. https://doi.org/10.1016/j.aquaeng.2015.07.002.

Cord-Ruwisch, R., 1985. A quick method for the determination of dissolved and precipitated sulfides in cultures of sulfate-reducing bacteria. J. Microbiol. Methods 4, 33–36. https://doi.org/10.1016/0167-7012(85)90005-3.

Doi, Y., Takaya, N., Takizawa, N., 2009. Novel denitrifying bacterium *Ochrobactrum anthropi* YD50.2 tolerates high levels of reactive nitrogen oxides. Appl. Environ. Microbiol. 75, 5186–5194. https://doi.org/10.1128/AEM.00604-09.

Drysdale, G.D., Kasan, H.C., Bux, F., 1999. Denitrification by heterotrophic bacteria during activated sludge treatment. Water SA 25, 357–362.

Espenberg, M., Truu, M., Mander, Ü., Kasak, K., Nõlvak, H., Ligi, T., Oopkaup, K., Maddison, M., Truu, J., 2018. Differences in microbial community structure and nitrogen cycling in natural and drained tropical peatland soils. art Sci. Rep. 8, 4742. https://doi.org/10.1038/s41598-018-23032-y.

Findlay, A.J., Gartman, A., MacDonald, D.J., Hanson, T.E., Shaw, T.J., Luther, G.W., 2014. Distribution and size fractionation of elemental sulfur in aqueous environments: the Chesapeake Bay and Mid-Atlantic Ridge. Geochem. Cosmochim. Acta 142, 334–348. https://doi.org/10.1016/j.gca.2014.07.032.

Gao, L., Zhou, W., Huang, J., He, S., Yan, Y., Zhu, W., Wu, S., Zhang, X., 2017. Nitrogen removal by the enhanced floating treatment wetlands from the secondary effluent. Bioresour. Technol. 234, 243–252. https://doi.org/10.1016/j.biortech.2017.03.036.

Griffiths, R.I., Whiteley, A.S., O'Donnell, A.G., Bailey, M.J., 2000. Rapid method for coextraction of DNA and RNA from natural environments for analysis of ribosomal DNA- and rRNA-based microbial community composition. Appl. Environ. Microbiol. 66, 5488–5491. https://doi.org/10.1128/AEM.66.12.5488-5491.2000.

Guo, G., Wu, D., Ekama, G.A., Ivleva, N.P., Hao, X., Dai, J., Cui, Y., Kumar Biswal, B., Chen, G., 2019. Investigation of multiple polymers in a denitrifying sulfur conversion-EBPR system. Water Res. 156, 179–187. https://doi.org/10.1016/j.watres.2019.03.025.

Hao, R., Meng, C., Li, J., 2017. Impact of operating condition on the denitrifying bacterial community structure in a 3DBER-SAD reactor. J. Ind. Microbiol. Biotechnol. 44, 9–21. https://doi.org/10.1007/s10295-016-1853-4.

Huang, S., Yu, D., Chen, G., Wang, Y., Tang, P., Liu, C., Tian, Y., Zhang, M., 2021. Realization of nitrite accumulation in a sulfide-driven autotrophic denitrification process: simultaneous nitrate and sulfur removal. art Chemosphere 278, 130413. https://doi.org/10.1016/j.chemosphere.2021.130413.

Huiliñir, C., Acosta, L., Yanez, D., Montalvo, S., Esposito, G., Retamales, G., Levicán, G., Guerrero, L., 2020. Elemental sulfur-based autotrophic denitrification in stoichiometric S^0/N ratio: calibration and validation of a kinetic model Calibration and validation of a kinetic model. art Bioresour. Technol. 307, 123229.

Janssen, A.J.H., Lettinga, G., de Keizer, A., 1999. Removal of hydrogen sulphide from wastewater and waste gases by biological conversion to elemental sulphur Colloidal and interfacial aspects of biologically produced sulphur particles. Colloids Surf., A 151, 389–397. https://doi.org/10.1016/S0927-7757(98)00507-X.

Kamyshny, A., Borkenstein, C.G., Ferdelman, T.G., 2009. Protocol for quantitative detection of elemental sulfur and polysulfide zero-valent sulfur distribution in natural aquatic samples. Geostand. Geoanal. Res. 33, 415–435. https://doi.org/10.1111/j.1751-908X.2009.00907.x.

Kiskira, K., Papirio, S., van Hullebusch, E.D., Esposito, G., 2017. Influence of pH, EDTA: Fe(II) ratio and microbial culture on Fe(II)-mediated autotrophic denitrification. Environ. Sci. Pollut. Res. 24, 21323–21333. https://doi.org/10.1007/s11356-017-9736-4.

Kostrytsia, A., Papirio, S., Frunzo, L., Mattei, M.R., Porca, E., Collins, G., Lens, P.N.L., Esposito, G., 2018a. Elemental sulfur-based autotrophic denitrification and denitritation: microbially catalyzed sulfur hydrolysis and nitrogen conversions. J. Environ. Manag. 211, 313–322. https://doi.org/10.1016/j.jenvman.2018.01.064.

Kostrytsia, A., Papirio, S., Mattei, M.R., Frunzo, L., Lens, P.N.L., Esposito, G., 2018b. Sensitivity analysis for an elemental sulfur-based two-step denitrification model. Water Sci. Technol. 78, 1296–1303. https://doi.org/10.2166/wst.2018.398.

Kostrytsia, A., Papirio, S., Morrison, L., Ijaz, U.Z., Collins, G., Lens, P.N.L., Esposito, G., 2018c. Biokinetics of microbial consortia using biogenic sulfur as a novel electron donor for sustainable denitrification. Bioresour. Technol. 270, 359–367. https://doi.org/10.1016/j.biortech.2018.09.044.

Lemaire, R., Thesing, G., Christensson, M., Zhao, H., Liviano, I., 2013. Experience from start-up and operation of deammonification MBBR plants, and testing of a new deammonification IFAS configuration. In: WEFTEC, pp. 1926–1947. https://doi.org/10.2175/193864713813673857.

Meyer, B., 1976. Elemental sulfur. Chem. Rev. 76, 367–388. https://doi.org/10.1021/cr60301a003.

Mora, M., Fernández, M., Gómez, J.M., Cantero, D., Lafuente, J., Gamisans, X., Gabriel, D., 2015. Kinetic and stoichiometric characterization of anoxic sulfide oxidation by SO-NR mixed cultures from anoxic biotrickling filters. Appl. Microbiol. Biotechnol. 99, 77–87. https://doi.org/10.1007/s00253-014-5688-5.

Namburath, M., Papirio, S., Moscariello, C., Di Costanzo, N., Pirozzi, F., Alappat, B.J., Sreekrishnan, T.R., 2020. Effect of nickel on the comparative performance of inverse fluidized bed and continuously stirred tank reactors for biogenic sulphur-driven autotrophic denitrification. art J. Environ. Manag. 275, 111301. https://doi.org/10.1016/j.jenvman.2020.111301.

Ødegaard, H., Rusten, B., Westrum, T., 1994. A new moving bed biofilm reactor - applications and results. Water Sci. Technol. 29, 157–165. https://doi.org/10.2166/wst.1994.0757.

Peng, C., Huang, H, Gao, Y, Fan, X, Peng, P., Zhang, X, Ren, H., 2021. A novel start-up strategy for mixotrophic denitrification biofilters by rhamnolipid and its performance on denitrification of low C/N wastewater. Chemosphere 239, 124726. https://doi.org/10.1016/j.chemosphere.2019.124726.

Piculell, M., Suarez, C., Li, C., Christensson, M., Persson, F., Wagner, M., Hermansson, M., Jönsson, K., Welander, T., 2016. The inhibitory effects of reject water on nitrifying populations grown at different biofilm thickness. Water Res. 104, 292–302. https://doi.org/10.1016/j.watres.2016.08.027.

Sahinkaya, E., Hasar, H., Kaksonen, A.H., Rittmann, B.E., 2011. Performance of a sulfide-oxidizing, sulfur-producing membrane biofilm reactor treating sulfide-containing bioreactor effluent. Environ. Sci. Technol. https://doi.org/10.1021/es200140c.

Sahinkaya, E., Kilic, A., Duygulu, B., 2014. Pilot and full scale applications of sulfur-based autotrophic denitrification process for nitrate removal from activated sludge process effluent. Water Res. 60, 210–217. https://doi.org/10.1016/j.watres.2014.04.052.

Sahinkaya, E., Yurtsever, A., Aktaş, Ö., Ucar, D., Wang, Z., 2015. Sulfur-based autotrophic denitrification of drinking water using a membrane bioreactor. Chem. Eng. J. 268, 180–186. https://doi.org/10.1016/j.cej.2015.01.045.

Sierra-Alvarez, R., Beristain-Cardoso, R., Salazar, M., Gómez, J., Razo-Flores, E., Field, J. A., 2007. Chemolithotrophic denitrification with elemental sulfur for groundwater treatment. Water Res. 41, 1253–1262. https://doi.org/10.1016/j.watres.2006.12.039.

Simard, M.-C., Masson, S., Mercier, G., Benmoussa, H., Blais, J.-F., Coudert, L., 2015. Autotrophic denitrification using elemental sulfur to remove nitrate from saline aquarium waters. J. Environ. Eng. 141. https://doi.org/10.1061/(ASCE)EE.1943-7870.0000977.

Ucar, D., Di Capua, F., Yücel, A., Nacar, T., Sahinkaya, E., 2021. Effect of nitrogen loading on denitrification, denitritation and filtration performances of membrane bioreactors fed with biogenic and chemical elemental sulfur. art Chem. Eng. J. 419, 129514. https://doi.org/10.1016/j.cej.2021.129514.

Ucar, D., Yilmaz, T., Di Capua, F., Esposito, G., Sahinkaya, E., 2020. Comparison of biogenic and chemical sulfur as electron donors for autotrophic denitrification in sulfur-fed membrane bioreactor (SMBR). art Bioresour. Technol. 299, 122574. https://doi.org/10.1016/j.biortech.2019.122574.

Wang, J., Ying, X., Huang, Y., Chen, Y., Shen, D., Zhang, X., Feng, H.J., 2021. Numerical study of hydrodynamic characteristics in a moving bed biofilm reactor. art Environ. Res. 194, 110614. https://doi.org/10.1016/j.envres.2020.110614.

Wang, J., Liu, X., Jiang, X., Zhang, L., Hou, C., Su, G., Wang, L., Mu, Y., Shen, J., 2020. Facilitated bio-mineralization of N,N-dimethylformamide in anoxic denitrification system: long-term performance and biological mechanism. art Water Res. 186, 116306. https://doi.org/10.1016/j.watres.2020.116306.

Wang, Y., Bott, C., Nerenberg, R., 2016. Sulfur-based denitrification: effect of biofilm development on denitrification fluxes. Water Res. 100, 184–193. https://doi.org/10.1016/j.watres.2016.05.020.

Welander, T., Piculell, M., 2016. Free-flowing Carrier Elements. WO 2015082349A1.

Xu, G., Peng, J., Feng, C., Fang, F., Chen, S., Xu, Y., Wang, X., 2015. Evaluation of simultaneous autotrophic and heterotrophic denitrification processes and bacterial community structure analysis. Appl. Microbiol. Biotechnol. 99, 6527–6536. https://doi.org/10.1007/s00253-015-6532-2.